(Rb) and poly (ADP-ribose) polymerase (PARP) were purchased from Cell Signaling (Beverly, MA). Cisplatin was purchased from Sigma Aldrich (St. Louis, MO). ECL Western blot detection system was purchased from GE Healthcare (Buckinghamshire, UK). Cell Proliferation ELISA (BrdU) was obtained from Roche Diagnostics Co (Indianapolis, IN). Alexa Fluor 488® conjugated donkey anti-mouse IgG antibodies and 4',6-diamidino-2-phenylindole (DAPI) were purchased from Invitrogen and Wako (Tokyo, Japan), respectively. p2'-(4-Hydroxyphenyl)-5-(4-methyl-1-piperazinyl)-2, 5'-bi-*1 H*-benzimidazole, trihydrochloride (Hoechst 33258) solution was purchased from Dojindo (Kumamoto, Japan). PI/RNase Staining Buffer was obtained from Becton Dickinson (Franklin Lakes, NJ). Other materials and chemicals were obtained from commercial sources.

Cell culture

SW480 and HT29 human colorectal cancer cells, that were obtained from American Type Culture Collection (Manassas, VA), were grown in Dulbecco's modified Eagle's medium (DMEM) (Invitrogen, San Diego, CA), containing 10% fetal calf serum (FCS) with penicillin (100 U/ml) and streptomycin (100 μg/ml) in a humidified 5% CO_2 incubator at 37°C. DLD-1 and HCT 116 human colorectal cancer cells were from American Type Culture Collection (Manassas, VA) and grown in Roswell Park Memorial Institute 1640 (RPMI) (Invitrogen, San Diego, CA) as described above.

UV-C exposure

UV-C exposure of cells was performed in UV-C 500 UV Crosslinker (8 W 254 nm UV lamp) (GE Healthcare), which creates CW light using 8 W 254 nm UV lamps. Fluorescent lamps without a phosphorescent coating emit UV with two peaks at 254 nm and 185 nm due to the peak emission of the mercury within the bulb. UV lamps used quartz (glass) block the 185 nm wavelength and emit only 254 nm UV. After aspiration of the growth medium, the cells were exposed to the indicated dose ($J/m^2 = 100$ $\mu J/cm^2$) of UV-C in 5 sec, and then incubated for the indicated times.

Cell proliferation assay

BrdU incorporation was measured using cell Proliferation ELISA (BrdU). The cells (7×10^3/well) were seeded onto 96-well plates and 48 h later, the cells were exposed to the indicated doses (0 or 10 J/m^2) of UV-C, just after the aspiration of the growth medium. The cells were then incubated in DMEM or RPMI medium with 1% FCS and 10 μM of cisplatin for 24 h. They were then used for the assay according to the manufacturer's protocol. All assays were done at least three times.

Cell cycle analysis

Cell cycle analysis was done as described previously [7]. In brief, SW480 cells were exposed to UV-C, followed by the incubation in DMEM with/without 10 μM of cisplatin for 96 h. The cells were then harvested and stained with 500 μl of PI/RNase staining buffer for 15 min at room temperature. They were finally analyzed by flow cytometry using a FACS Calibur instrument (Becton Dickinson); data were analyzed using the CELL Quest computer program (Becton Dickinson) as previously described. All data were obtained from at least three independent experiments.

Colony formation assay

Human colorectal cancer cells (SW480, DLD-1, HT29 and HCT116) were exposed to UV-C and then incubated in DMEM or RPMI medium and with/without 10 μM of cisplatin. Twenty four h after treatment, the cells were trypsinized and the cells (3×10^3) were reseeded into fresh tissue culture dishes and incubated for 7 days. Fresh media were added at day 4. At day 7, the media were removed and the cells were fixed with 2 ml of clonogenic reagent (50% ethanol, 0.25% 1,9-dimethylmethylene blue) for 45 min. They were then washed with PBS twice and counted the blue colonies on 5 randomly chosen fields.

Western blotting

The cells were lysed in lysis buffer [20 mM Tris/HCl (pH 7.5), 150 mM NaCl, 1 mM EDTA, 1 mM EGTA, 1% TritonX-100, 2.5 mM sodium pyrophosphate, 50 mM NaF, 50 mM HEPES, 1 mM Na_3VO_4 and 2 mM phenylmethylsulfonyl fluoride (PMSF)] and scraped from the Petri dishes. Protein extracts were examined by Western blot analysis as previously described [49,50].

Immunofluorescence microscopy studies

Immunofluorescence microscopy studies were performed as described previously [46]. Live cells grown on coverslip-bottom dishes in DMEM were first exposed to the mouse anti-EGFR antibody that recognized the extracellular domain of EGFR for 15 min and then exposed to UV-C (10 J/m^2) and/or cisplatin (10 μM) and incubated in DMEM for the indicated times (0.5 h, 6 h, 12 h and 24 h) at 37°C. They were then fixed with 4% paraformaldehyde for 10 min on ice and then exposed to 0.1% Triton X-100 for 10 min to permeabilize the cell membrane. They were followed by exposure to Alexa Fluor 488® conjugated donkey anti-mouse IgG antibodies (green signal) and 4',6-diamidino-2-phenylindole (DAPI) for 1 h. The cells were then examined by fluorescence microscopy, BIOREVO (BZ-9000) (Keyence, Tokyo, Japan) according to the manufacturer's protocol.

Quantification of cell surface EGFR by enzyme-linked immunosorbent assay (ELISA)

Quantification of cell surface EGFR was performed as described previously [26]. In brief, SW480 cells were first exposed to the mouse anti-EGFR antibody in DMEM containing 1% BSA, for 15 min at 37°C. The cells were then incubated for the indicated times in DMEM with/without 10 μM of cisplatin after exposure to UV-C, then fixed with 4% paraformaldehyde for 10 min on ice. After blocking with 1% BSA in PBS for 1 h, the cells were exposed to an anti-mouse IgG, horseradish peroxidase-linked whole antibody (GE healthcare, Piscataway, NJ) for 1 h at room temperature, followed by washing four times with PBS containing 1% BSA. Finally, the cells were exposed to 50 μl of 1-stepTM Ultra TMB-ELISA reagent (Pierce, Rockford, IL) for 5 min at room temperature. The absorbance of each sample at 450 nm was then measured.

Hoechst 33258 staining

Live cells grown on coverslip-bottom dishes were first exposed to UV-C (10 J/m^2) and/or cisplatin (10 μM) for 72 h and then stained with Hoechst 33258 in DMEM without FCS for 1 h at 37°C. They were then fixed with 4% paraformaldehyde for 10 min on ice. The cells were then examined by fluorescence microscopy, as described above.

Densitometric analysis

The densitometric analysis was performed using scanner and image analysis software (Image J ver. 1.45 g). The back ground subtracted signal intensity of each protein signal was normalized by the respective control signal. All data were obtained from at least three independent experiments.

Statistical analysis

The data were analyzed by ANOVA followed by Bonferroni method for multiple comparisons between the indicated pairs, and a $p < 0.05$ was considered significant.

Additional file

Additional file 1: Effect of 10 J/m^2 UV-C on HER2, EGFR, phospho-Rb and cyclin D1 in human colorectal cancer cells. SW480, DLD-1, HT29 and HCT116 cells were exposed to 10 J/m^2 of UV-C and then treated for the indicated periods. Protein extracts were then harvested and examine by Western blotting using anti-HER2, anti-EGFR, anti-phospho-Rb, anti-cyclin D1 and anti-GAPDH antibodies.

Abbreviations

UV-C: Ultra-violet-C; RTKs: Receptor tyrosine kinases; EGF: Epidermal growth factor; EGFR: EGF receptor; HER2: Human epidermal growth factor receptor-2; GAPDH: Glyceraldehyde-3-phosphate dehydrogenase; Rb: Retinoblastoma protein; PARP: Poly (ADP-ribose) polymerase; MAPK: Mitogen-activated protein kinase; GSK: Glycogen synthase kinas; DMEM: Dulbecco's modified Eagle's medium; RPMI: Roswell Park Memorial Institute 1640; FCS: Fetal calf serum; PBS: Phosphate buffered saline; BrdU: Bromodeoxyuridine (5-bromo-2'-deoxyuridine); ELISA: Enzyme-linked immunosorbent assay; DAPI: 4',6-diamidino-2-phenylindole; Hoechst 33258: p2'-(4-Hydroxyphenyl)-5-(4-methyl-1-piperazinyl)-2, 5'-bi-*1H*-benzimidazole, trihydrochloride.

Competing interests

The authors declare that they have no competing interests.

Authors' contributions

SA designed the research studies; SA, JK, TY, MN, TO, MS, TY and MI carried out the molecular biological studies; SA, IY, OK and HM analyzed and interpreted the data; JK wrote the draft of the manuscript. All authors read and approved the final manuscript.

Acknowledgements

We are very grateful to Ms. Yoko Kawamura for her skillful technical assistance. This work was supported in part by Grant-in-Aid for Scientific Research (22790639 to S.A) from the Ministry of Education, Science, Sports and Culture of Japan.

Author details

[1]Departments of Gastroenterology, Gifu University Graduate School of Medicine, Gifu 501-1194, Japan. [2]Departments of Pharmacology, Gifu University Graduate School of Medicine, Gifu 501-1194, Japan. [3]1-1 Yanagido, Gifu 501-1194, Japan.

Received: 1 February 2012 Accepted: 24 April 2012
Published: 12 July 2012

References

1. Hynes NE, Horsch K, Olayioye MA, Badache A: **The ErbB receptor tyrosine family as signal integrators.** *Endocr Relat Cancer* 2001, **8**:151–159.
2. Kuan CT, Wikstrand CJ, Bigner DD: **EGF mutant receptor vIII as a molecular target in cancer therapy.** *Endocr Relat Cancer* 2001, **8**:83–96.
3. Zandi R, Larsen AB, Andersen P, Stockhausen MT, Poulsen HS: **Mechanisms for oncogenic activation of the epidermal growth factor receptor.** *Cell Signal* 2007, **19**:2013–2023.
4. Nakashima M, Adachi S, Yasuda I, Yamauchi T, Kozawa O, Moriwaki H: **Rho-kinase regulates negatively the epidermal growth factor-stimulated colon cancer cell proliferation.** *Int J Oncol* 2010, **36**:585–592.
5. Borg A, Linell F, Idvall I, Johansson S, Sigurdsson H, Ferno M, Killander D: **HER2/neu amplification and comedo type breast carcinoma.** *Lancet* 1989, **1**:1268–1269.
6. Shepard HM, Lewis GD, Sarup JC, Fendly BM, Maneval D, Mordenti J, Figari I, Kotts CE, Palladino MA Jr, Ullrich A, *et al*: **Monoclonal antibody therapy of human cancer: taking the HER2 protooncogene to the clinic.** *J Clin Immunol* 1991, **11**:117–127.
7. Shimizu M, Deguchi A, Lim JT, Moriwaki H, Kopelovich L, Weinstein IB: **(–)-Epigallocatechin gallate and polyphenon E inhibit growth and activation of the epidermal growth factor receptor and human epidermal growth factor receptor-2 signaling pathways in human colon cancer cells.** *Clin Cancer Res* 2005, **11**:2735–2746.
8. Feng FY, Varambally S, Tomlins SA, Chun PY, Lopez CA, Li X, Davis MA, Chinnaiyan AM, Lawrence TS, Nyati MK: **Role of epidermal growth factor receptor degradation in gemcitabine-mediated cytotoxicity.** *Oncogene* 2007, **26**:3431–3439.
9. Masuda M, Suzui M, Weinstein IB: **Effects of epigallocatechin-3-gallate on growth, epidermal growth factor receptor signaling pathways, gene expression, and chemosensitivity in human head and neck squamous cell carcinoma cell lines.** *Clin Cancer Res* 2001, **7**:4220–4229.
10. Siddik ZH: **Cisplatin: mode of cytotoxic action and molecular basis of resistance.** *Oncogene* 2003, **22**:7265–7279.
11. Parker LJ, Italiano LC, Morton CJ, Hancock NC, Ascher DB, Aitken JB, Harris HH, Campomanes P, Rothlisberger U, De Luca A, *et al*: **Studies of glutathione transferase P1-1 bound to a platinum(IV)-based anticancer compound reveal the molecular basis of its activation.** *Chemistry* 2011, **17**:7806–7816.
12. Musceila A, Urso L, Calabriso N, Vetrugno C, Fanizzi FP, Storelli C, Marsigliante S: **Functions of epidermal growth factor receptor in cisplatin response of thyroid cells.** *Biochem Pharmacol* 2009, **77**:979–992.

13. Ahsan A, Hiniker SM, Ramanand SG, Nyati S, Hegde A, Helman A, Menawat R, Bhojani MS, Lawrence TS, Nyati MK: **Role of epidermal growth factor receptor degradation in cisplatin-induced cytotoxicity in head and neck cancer.** *Cancer Res* 2010, **70**:2862–2869.
14. Winograd-Katz SE, Levitzki A: **Cisplatin induces PKB/Akt activation and p38 (MAPK) phosphorylation of the EGF receptor.** *Oncogene* 2006, **25**:7381–7390.
15. Benhar M, Dalyot I, Engelberg D, Levitzki A: **Enhanced ROS production in oncogenically transformed cells potentiates c-Jun N-terminal kinase and p38 mitogen-activated protein kinase activation and sensitization to genotoxic stress.** *Mol Cell Biol* 2001, **21**:6913–6926.
16. Latonen L, Laiho M: **Cellular UV damage responses-functions of tumor suppressor p53.** *Biochim Biophys Acta* 2005, **1755**:71–89.
17. Olsen BB, Neves-Petersen MT, Klitgaard S, Issinger OG, Petersen SB: **UV light blocks EGFR signalling in human cancer cell lines.** *Int J Oncol* 2007, **30**:181–185.
18. Kim SC, Park SS, Lee YJ: **Effect of UV irradiation on colorectal cancer cells with acquired TRAIL resistance.** *J Cell Biochem* 2008, **104**:1172–1180.
19. Petersen MT, Jonson PH, Petersen SB: **Amino acid neighbours and detailed conformational analysis of cysteines in proteins.** *Protein Eng* 1999, **12**:535–548.
20. Prompers JJ, Hilbers CW, Pepermans HA: **Tryptophan mediated photoreduction of disulfide bond causes unusual fluorescence behaviour of Fusarium solani pisi cutinase.** *FEBS Lett* 1999, **456**:409–416.
21. Neves-Petersen MT, Gryczynski Z, Lakowicz J, Fojan P, Pedersen S, Petersen E, Bjorn Petersen S: **High probability of disrupting a disulphide bridge mediated by an endogenous excited tryptophan residue.** *Protein Sci* 2002, **11**:588–600.
22. Vanhooren A, Devreese B, Vanhee K, Van Beeumen J, Hanssens I: **Photoexcitation of tryptophan groups induces reduction of two disulfide bonds in goat alpha-lactalbumin.** *Biochemistry* 2002, **41**:11035–11043.
23. Neves-Petersen MT, Snabe T, Klitgaard S, Duroux M, Petersen SB: **Photonic activation of disulfide bridges achieves oriented protein immobilization on biosensor surfaces.** *Protein Sci* 2006, **15**:343–351.
24. Neves-Petersen MT, Duroux M, Skovsen E, Duroux L, Petersen SB: **Printing novel molecular architectures with micrometer resolution using light.** *J Nanosci Nanotechnol* 2009, **9**:3372–3381.
25. Neves-Petersen MT, Klitgaard S, Pascher T, Skovsen E, Polivka T, Yartsev A, Sundstrom V, Petersen SB: **Flash photolysis of cutinase: identification and decay kinetics of transient intermediates formed upon UV excitation of aromatic residues.** *Biophys J* 2009, **97**:211–226.
26. Adachi S, Yasuda I, Nakashima M, Yamauchi T, Kawaguchi J, Shimizu M, Itani M, Nakamura M, Nishii Y, Yoshioka T, *et al*: **Ultraviolet irradiation can induce evasion of colon cancer cells from stimulation of epidermal growth factor.** *J Biol Chem* 2011, **286**:26178–26187.
27. Sorenson CM, Barry MA, Eastman A: **Analysis of events associated with cell cycle arrest at G2 phase and cell death induced by cisplatin.** *J Natl Cancer Inst* 1990, **82**:749–755.
28. Sherr CJ: **Cancer cell cycles.** *Science* 1996, **274**:1672–1677.
29. Hoffman RM: **In vitro sensitivity assays in cancer: a review, analysis, and prognosis.** *J Clin Lab Anal* 1991, **5**:133–143.
30. Boulares AH, Yakovlev AG, Ivanova V, Stoica BA, Wang G, Iyer S, Smulson M: **Role of poly(ADP-ribose) polymerase (PARP) cleavage in apoptosis. Caspase 3-resistant PARP mutant increases rates of apoptosis in transfected cells.** *J Biol Chem* 1999, **274**:22932–22940.
31. Kapitanovic S, Radosevic S, Kapitanovic M, Andelinovic S, Ferencic Z, Tavassoli M, Primorac D, Sonicki Z, Spaventi S, Pavelic K, Spaventi R: **The expression of p185(HER-2/neu) correlates with the stage of disease and survival in colorectal cancer.** *Gastroenterology* 1997, **112**:1103–1113.
32. Mendelsohn J, Baselga J: **The EGF receptor family as targets for cancer therapy.** *Oncogene* 2000, **19**:6550–6565.
33. Zwang Y, Yarden Y: **p38 MAP kinase mediates stress-induced internalization of EGFR: implications for cancer chemotherapy.** *Embo J* 2006, **25**:4195–4206.
34. Ciccarelli RB, Solomon MJ, Varshavsky A, Lippard SJ: **In vivo effects of cis- and trans-diamminedichloroplatinum(II) on SV40 chromosomes: differential repair, DNA-protein cross-linking, and inhibition of replication.** *Biochemistry* 1985, **24**:7533–7540.
35. Salles B, Butour JL, Lesca C, Macquet JP: **cis-Pt(NH3)2Cl2 and trans-Pt(NH3) 2Cl2 inhibit DNA synthesis in cultured L1210 leukemia cells.** *Biochem Biophys Res Commun* 1983, **112**:555–563.
36. Mello JA, Lippard SJ, Essigmann JM: **DNA adducts of cis-diamminedichloroplatinum(II) and its trans isomer inhibit RNA polymerase II differentially in vivo.** *Biochemistry* 1995, **34**:14783–14791.
37. Sorenson CM, Eastman A: **Influence of cis-diamminedichloroplatinum(II) on DNA synthesis and cell cycle progression in excision repair proficient and deficient Chinese hamster ovary cells.** *Cancer Res* 1988, **48**:6703–6707.
38. Nakashima M, Adachi S, Yasuda I, Yamauchi T, Kawaguchi J, Hanamatsu T, Yoshioka T, Okano Y, Hirose Y, Kozawa O, Moriwaki H: **Inhibition of Rho-associated coiled-coil containing protein kinase enhances the activation of epidermal growth factor receptor in pancreatic cancer cells.** *Mol Cancer* 2011, **10**:79.
39. Benhar M, Engelberg D, Levitzki A: **Cisplatin-induced activation of the EGF receptor.** *Oncogene* 2002, **21**:8723–8731.
40. Yoshida T, Okamoto I, Iwasa T, Fukuoka M, Nakagawa K: **The anti-EGFR monoclonal antibody blocks cisplatin-induced activation of EGFR signaling mediated by HB-EGF.** *FEBS Lett* 2008, **582**:4125–4130.
41. Douillard JY, Siena S, Cassidy J, Tabernero J, Burkes R, Barugel M, Humblet Y, Bodoky G, Cunningham D, Jassem J, *et al*: **Randomized, phase III trial of panitumumab with infusional fluorouracil, leucovorin, and oxaliplatin (FOLFOX4) versus FOLFOX4 alone as first-line treatment in patients with previously untreated metastatic colorectal cancer: the PRIME study.** *J Clin Oncol* 2010, **28**:4697–4705.
42. Siena S, Peeters M, Van Cutsem E, Humblet Y, Conte P, Bajetta E, Comandini D, Bodoky G, Van Hazel G, Salek T, *et al*: **Association of progression-free survival with patient-reported outcomes and survival: results from a randomised phase 3 trial of panitumumab.** *Br J Cancer* 2007, **97**:1469–1474.
43. Amado RG, Wolf M, Peeters M, Van Cutsem E, Siena S, Freeman DJ, Juan T, Sikorski R, Suggs S, Radinsky R, *et al*: **Wild-type KRAS is required for panitumumab efficacy in patients with metastatic colorectal cancer.** *J Clin Oncol* 2008, **26**:1626–1634.
44. Countaway JL, Nairn AC, Davis RJ: **Mechanism of desensitization of the epidermal growth factor receptor protein-tyrosine kinase.** *J Biol Chem* 1992, **267**:1129–1140.
45. Theroux SJ, Latour DA, Stanley K, Raden DL, Davis RJ: **Signal transduction by the epidermal growth factor receptor is attenuated by a COOH-terminal domain serine phosphorylation site.** *J Biol Chem* 1992, **267**:16620–16626.
46. Adachi S, Shimizu M, Shirakami Y, Yamauchi J, Natsume H, Matsushima-Nishiwaki R, To S, Weinstein IB, Moriwaki H, Kozawa O: **(−)-Epigallocatechin gallate downregulates EGF receptor via phosphorylation at Ser1046/1047 by p38 MAPK in colon cancer cells.** *Carcinogenesis* 2009, **30**:1544–1552.
47. Adachi S, Yasuda I, Nakashima M, Yamauchi T, Yamauchi J, Natsume H, Moriwaki H, Kozawa O: **HSP90 inhibitors induce desensitization of EGF receptor via p38 MAPK-mediated phosphorylation at Ser1046/1047 in human pancreatic cancer cells.** *Oncol Rep* 2010, **23**:1709–1714.
48. Kartalou M, Essigmann JM: **Mechanisms of resistance to cisplatin.** *Mutat Res* 2001, **478**:23–43.
49. Adachi S, Nagao T, Ingolfsson HI, Maxfield FR, Andersen OS, Kopelovich L, Weinstein IB: **The inhibitory effect of (−)-epigallocatechin gallate on activation of the epidermal growth factor receptor is associated with altered lipid order in HT29 colon cancer cells.** *Cancer Res* 2007, **67**:6493–6501.
50. Adachi S, Nagao T, To S, Joe AK, Shimizu M, Matsushima-Nishiwaki R, Kozawa O, Moriwaki H, Maxfield FR, Weinstein IB: **(−)-Epigallocatechin gallate causes internalization of the epidermal growth factor receptor in human colon cancer cells.** *Carcinogenesis* 2008, **29**:1986–1993.

doi:10.1186/1476-4598-11-45
Cite this article as: Kawaguchi *et al.*: Cisplatin and ultra-violet-C synergistically down-regulate receptor tyrosine kinases in human colorectal cancer cells. *Molecular Cancer* 2012 **11**:45.

The Prostate 72:533–541 (2012)

Organ Specific Gst-pi Expression of the Metastatic Androgen Independent Prostate Cancer Cells in Nude Mice

Taku Naiki,[1,2] Makoto Asamoto,[1]* Naomi Toyoda-Hokaiwado,[1] Aya Naiki-Ito,[1] Keiichi Tozawa,[2] Kenjiro Kohri,[2] Satoru Takahashi,[1] and Tomoyuki Shirai[1]

[1]*Department of Experimental Pathology and Tumor Biology, Nagoya City University, Graduate School of Medical Sciences, Nagoya, Japan*

[2]*Department of Nephro-urology, Nagoya City University, Graduate School of Medical Sciences, Nagoya, Japan*

BACKGROUND. Elucidating the mechanisms of metastasis in prostate cancer, particularly to the bone, is a major issue for treatment of this malignancy. We previously reported that an androgen-independent variant had higher expression of glutathione S-transferase pi (Gst-pi) compared with a parent androgen-dependent transplantable rat prostate carcinoma which was established from the transgenic rat for adenocarcinoma of the prostate (TRAP).

METHODS. A new cell line, PCai1, was established from the androgen-independent tumor and investigated its metastatic potential in nude mice. The tumorigenesis of PCai1 cells in vivo was studied by subcutaneous transplantations into nude mice. The growth in the micro-environment of the prostate was studied by orthotopic transplantation of PCai1 cells into nude mice. The metastatic potential of PCai1 cells was studied by tail vein injections. Effects of *Gst-pi* knocked down were analysis in PCai1 cells.

RESULTS. PCai1 frequently formed metastatic lesions in the lung and lymph nodes after orthotopic implantation in the prostate. Intravenous injections of PCai1, metastasis to lung and bone were obvious. PCai1 had strong expression for Gst-pi, therefore we tried knocked down *Gst-pi*. *Gst-pi*-siRNA in vitro significantly suppressed cell proliferation rate. In addition, high levels of intracellular reactive oxygen species (ROS) were recognized in the *Gst-pi* knockout.

CONCLUSIONS. Gst-pi expression of the prostate cancers are dependent on metastatic site, and that Gst-pi has an important role in adapting prostate cancer for growth and metastasis involving an alteration of ROS signals. *Prostate 72: 533–541, 2012.* © 2011 Wiley Periodicals, Inc.

KEY WORDS: **prostate cancer; metastasis; Gst-pi; rats; cell line**

INTRODUCTION

Prostate cancer is one of the most frequently diagnosed cancers in the Western world [1]. Because prostate cancer development is initially androgen dependent, the basic therapeutic strategy has been the deprivation of androgens [2]. However, most tumors ultimately relapse after a period of initial response to this therapy and progress to castration-resistant prostate cancer (CRPC), for which effective therapeutic procedures are extremely limited. Administration of docetaxel has been established as a new standard of chemotherapy for CRPC patients [3–5]. However, it is not curative, and optimal timing of administration remains controversial. Consequently, there is a need

Grant sponsor: Ministry of Education, Culture, Sports Science and Technology of Japan; Grant sponsor: Ministry of Health, Labor and Welfare of Japan; Grant sponsor: Ono Pharmaceutical Co., Ltd.

Disclosure: There are no potential conflicts of interest.

Naomi Toyoda-Hokaiwado's present address is Division of Genetics and Mutagenesis, National Institute of Health Sciences, Tokyo, Japan.

*Correspondence to: , Dr. Makoto Asamoto, MD, PhD, Department of Experimental Pathology and Tumor Biology, Nagoya City University, Graduate School of Medical Sciences, Kawasumi 1, Mizuho-cho, Mizuho-ku 467-8601, Nagoya, Japan.
E-mail: masamoto@med.nagoya-cu.ac.jp

Received 7 January 2011; Accepted 15 June 2011
DOI 10.1002/pros.21455
Published online 11 July 2011 in Wiley Online Library (wileyonlinelibrary.com).

for exploration of new therapeutic strategies targeting detailed molecular mechanisms for the development of castration resistance in prostate cancer.

The generation of suitable in vivo models is essential to gain a better understanding of the processes associated with the development and progression of prostate cancer [6,7]. We previously reported on the transgenic rat model for adenocarcinoma of the prostate (TRAP) model [8], which features the introduction of the SV40 T antigen (SV40 Tag) gene under probasin control. In this model, complete androgen-dependent prostate adenocarcinomas developed in 100% of animals by 15 weeks of age [8–10]. These tumors were transplantable into the subcutis of nude mice. The transplanted tumors expressing androgen receptor (AR) regressed soon after the mice were castrated, but resumed growth under androgen depletion 12 weeks later. As the sequential changes of the xenograft resemble the clinical behavior of prostate cancer, this model may provide an excellent system to study the mechanisms associated with castration-resistant progression of prostate cancer and to evaluate new modalities for CRPC [11]. The androgen-independent prostate tumors established under such an experimental condition were subjected to cDNA microarray analysis which showed that glutathione S-transferase pi (*Gst-pi*) was overexpressed compared to the androgen-dependent tumors. Glutathione S-transferase pi (*GST-pi*) was also found to be overexpressed in the androgen-independent prostate cancer cell line, PC3 [11]. The suppression of GST-pi expression by siRNA inhibited tumor growth after subcutaneous transplantation of PC3 cells in nude mice [11].

A major component involved in the maintenance of reduction-oxidation (redox) balance in the cell is the glutathione redox system. Methods of inactivating *GST-pi* had been identified in almost all of the prostate cancer cases examined by Nelson et al. [12]. Since then, many reports have described the relations between *GST-pi* and androgen-dependent prostate cancer, and loss of the expression of their promoter sequences by methylation was found as an early event in human prostate carcinogenesis [13,14]. Therefore, a sensitive balance appears to exist between the oxidant and antioxidant components of the cells and their regulatory mechanisms in developing a malignant state in prostate tissue.

Redox reactions that generate reactive oxygen species (ROS) such as hydrogen peroxide, superoxide, and hydroxyl-free radicals have been identified as important chemical mediators in the regulation of signal transduction processes involved in cell growth and differentiation and have been reviewed [15–17]. ROS content is relatively higher in prostate epithelial cells than in most other tissues [18]. Direct evidence linking ROS with an increase in tumor development in the prostate has been established [19,20]. Previous studies highlighted the altered pro-oxidant–antioxidant status in prostatic tissue, and also in cell lines where the imbalance between these antagonists played a major role in the initiation of prostate carcinogenesis [21]. However, only few reports are available that describes interactions between androgen-independent prostate cancer and ROS. Moreover, no report addressed the mechanism using a cell line with a high metastatic potential in vivo.

In the present study, new androgen-independent prostate cancer cells were established which metastasized when transplanted into nude mice. The expression and function of Gst-pi in each metastatic site of the androgen-independent prostate cancer cells were studied.

MATERIALS AND METHODS

A New Androgen-Independent Prostate Cancer Cell Line

Cultures were initiated by mechanical disruption of the androgen-independent prostate tumor in nude mice [11] followed by enzymatic digestion with trypsin for 24 hr at 37°C. The resulting cells were incubated in DMEM (Nissui, Tokyo, Japan) with 10% heat-inactivated fetal bovine serum (FBS) (Equitech-Bio, Kerrville, TX). After 10 months passage and incubation, the surviving cells were selected and the cells that had the SV40 Tag expressions by RT-PCR were subcloned. Furthermore, the surviving cells in the androgen depleted medium containing 10% charcoal-stripped- (CS-) FBS (Hyclone) were selected, and one of these cell lines, named PCai1, which was androgen-independent cell line in vitro was used in our experiments. All cell cultures were maintained at 37°C in a humidified incubator with an atmosphere of 5% CO_2/95% air.

In Vivo Tumor Growth

Six-week-old male KSN/nu-nu nude mice were obtained from Nippon SLC. Mice were maintained in plastic cages on hardwood chips in an air-conditioned, pathogen-free animal room at 22 ± 2°C and 50% humidity with 12:12 hr light/dark cycle. All animal experiments were performed under protocols approved by the Institutional Animal Care and Use Committee of Nagoya City University School of Medical Sciences.

Subcutaneous transplantation of PCai1 cells. The tumorigenesis of PCai1 cells in vivo was studied by

subcutaneous transplantations into nude mice. PCai1 cells were cultured in T-75 flasks to confluence, trypsinized, and enumerated. Under isoflurane anesthesia four mice were surgically castrated and after 3 days, 1×10^5 PCai1 cells were injected subcutaneously into four normal and four castrated mice. Tumor sizes were calculated every 2 weeks, and mice were sacrificed 10 weeks after the implantation.

Orthotopic transplantation of PCai1 cells. The growth in the microenvironment of the prostate was studied by orthotopic transplantation of PCai1 cells into nude mice. Under isoflurane anesthesia, 5 of 10 nude mice were surgically castrated. After 3 days, 5×10^5 PCai1 cells were implanted into the lateral lobe of the prostate in both castrated and non-castrated mice. Two mice of each group were sacrificed 2 weeks after the injection. The study was terminated until become when the mice appeared moribund. After sacrifice, the orthotopic growth of the tumor and metastases in the para-aortic and bilateral inguinal lymph nodes, lung and systemic bone tissues were investigated histopathologically, as well as performing immunohistochemical analyses for AR, SV40 Tag, and Gst-pi.

Tail vein injection of PCai1 cells. The metastatic potential of PCai1 cells was studied by tail vein injections. Seven $\times 10^6$ cells were injected into the tail veins of 10 mice under anesthesia. At 5 and 9 weeks after the injections, the mice were sacrificed and the metastases in the para-aortic and bilateral inguinal lymph nodes, lung and systemic bone were investigated macroscopically and by immunohistochemical staining.

Histopathological Analysis

The transplants and metastatic tumors were fixed in 10% buffered formalin and embedded in paraffin. For bone metastases, specimens were treated with sterile decalcification solution for 48 hr prior to paraffin embedding. Serial (4 μm thick) sections were prepared. For immunohistochemical analysis, deparaffinized sections of the tissues were incubated with 1:1,000 diluted anti-Gst-pi (MBL, Nagoya, Japan), 1:100 diluted anti-AR (Santa Cruz Biotechnology, Inc., CA), 1:500 diluted SV40 Tag antibody (PharMingen, San Diego, CA). Antibody binding was visualized by a conventional immunostaining method using an autoimmunostaining apparatus (HX System, Ventana, Tucson, AZ).

RNA Preparation and Quantitative RT-PCR for Gst-pi and Gapdh

Total RNA was extracted using Isogen (Nippon Gene, Tokyo, Japan). One microgram sample was converted to complementary DNA with avian myoblastosis virus reverse transcriptase and oligo dT primers (TaKaRa, Otsu, Japan) in 20 μl of reaction mixture and 2 μl aliquots were subjected to quantitative polymerase chain reaction in 20 μl reactions using SYBR Premix Ex Taq™ (TaKaRa) and a Light Cycler apparatus (Roche Diagnostics, Mannheim, Germany). The fluorescence intensity of double-strand-specific SYBR Green 1, reflecting the amount of formed polymerase chain reaction product, was monitored at the end of each elongation step. Cyclophilin messenger RNA levels were employed to normalize for the 5′ sample complementary DNA content. Primer sequences for rat *Gst-pi* were 5′-GCTCTTT-AGGGCTTTATGGG-3′ and 5′-CTGTTTACCATT-GCCGTTGA-3′, and 5′-GCATCCTGCACCACCAA-CTG-3′ and 5′-GCCTGCTTCACCACCTTCTT-3′ for glyceraldehyde-3-phosphate dehydrogenase (*Gapdh*). Initial denaturation was at 95°C for 5 sec, annealing was at 55°C for 15 sec, and subsequently elongation was at 72°C for 30 sec. Gapdh mRNA levels were used for normalizing the sample cDNA content of PCai1 cells.

siRNA Transfection and Cell Growth Assay In Vitro

Stealth Select RNAi targeting rat *Gst-pi* sequences were obtained from Invitrogen. PCai1 cells (2×10^5) were seeded in six-well plates and transfected with 30 nM siRNA using LipofectAMINE RNAiMAX (Invitrogen) according to the manufacturer's protocol. Silencer negative control #1 siRNA (Invitrogen) with no significant homology to any known rat genes was used as a negative control siRNA. The ability of siRNA to silence the expression level of *Gst-pi* mRNA was checked on the second day after transfection. For monitoring growth inhibition, cells were trypsinized ($n = 4$) on days 3 and 5, and then the cell numbers were counted.

In Vivo Tumor Growth Analysis by Using siRNA for *Gst-pi*

Twenty-four hours after *Gst-pi* siRNA transfection by lipofectamine in T-75 flask, PCai1 cells were trypsinized and suspended in the DMEM media without serum, and 1×10^5/mouse cells were injected subcutaneously into five normal and five castrated nude mice. Negative control siRNA treated cells were also injected into normal and castrated mice for controls. Tumor volume was calculated every week, and 3 weeks after inoculation, the four groups of mice

were sacrificed and the final tumor volumes were measured in each group.

Western Blotting for Gst-pi and AR

Cells were lysed in SDS buffer and 10 μl were resolved on 12% polyacrylamide gels and transferred to Hybond ECL (GE Healthcare). Gst-pi and AR expression levels were assessed with the same antibody used for immunohistochemical staining. Beta actin expression was evaluated to confirm equal amount of protein loadings by monoclonal anti-beta-actin (Sigma, St. Louis, MO).

Cell Proliferation Assay After Dihydrotestosterone (DHT) Treatment

PCai1 cells were pretreated with medium containing CS-FBS for 2 weeks, and cell proliferation was measured in response to dihydrotestosterone (DHT) (Wako, Tokyo, Japan) treatments. PCai1 cells (5×10^4) were re-seeded in 96-well plates and treated with DHT from 10^{-5} to 10^5 nM in CS-FBS medium. Twenty-four hours after incubation, 10 μl/well of Cell Proliferation Reagent WST-1 (Roche, Basal, Switzerland) was added to the cells. Two hours after incubation, increase in fluorescence was measured by Spectrafluor Plus (Wako). The mean fluorescence intensity at 430 nm was calculated.

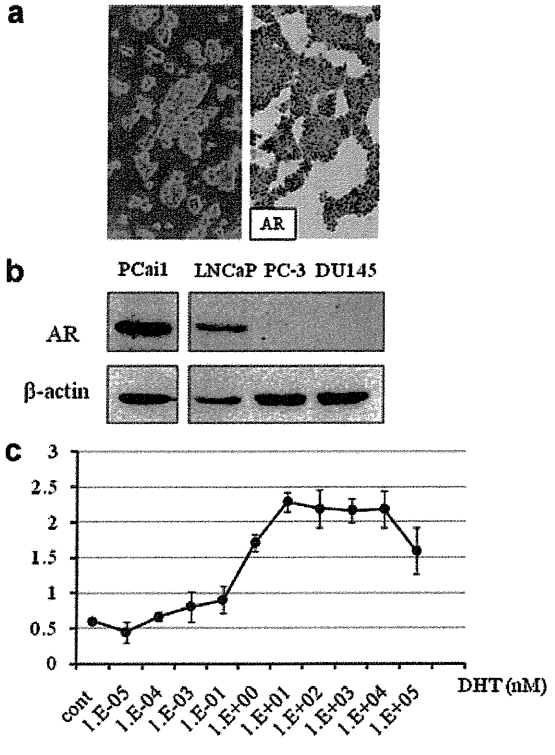

Fig. 1. Androgen receptor expression and function in PCai1 cell line. The established cell line, PCai1, grew with spheroid formation, and immunohistochemical analysis revealed intense nuclear staining for AR in androgen containing medium (**a**). Western blot analysis showed that PCai1 cells had AR expression similar to the human prostate cancer cell line LNCaP (**b**). WST-1 assay revealed that growth of PCai1 cells in CS-FBS medium was enhanced by 1–10 nM dihydrotestosterone (DHT) (**c**). [Color figure can be seen in the online version of this article, available at http://wileyonlinelibrary.com/journal/pros]

Measurement of Intracellular ROS Level

After pretreatment with DMEM without phenol red for 24 hr, 1×10^4 PCai1 cells were re-seeded in 96-well plates for 24 hr. The cells were then treated with 100 μg/ml 5-(and-6-)-chloromethyl-2′, 7′-dichlorodihydrofluorescein diacetate, acetyl ester (CM-H_2DCFDA) dye (Invitrogen). After 45 min incubation in the dark, levels of specific fluorescence were measured by Spectrafluor Plus. The data were normalized by the proliferation rate measured by the WST-1 assay.

Ethacrynic Acid Treatment in PCai1 Cells

To examine direct effects of Gst-pi on production of ROS or cell proliferation, PCai1 cells were treated with ethacrynic acid (EA) (Sigma), glutathione S-transferase pi inhibitor. Briefly, PCai1 cells were pretreated with phenol-free medium containing 10% FBS for 2 weeks, and cell proliferation and intracellular ROS were measured in response to EA treatments. PCai1 cells (1×10^5) were seeded in six-well plates, and exposed to 1 μM, 10 μM of EA. Cells were

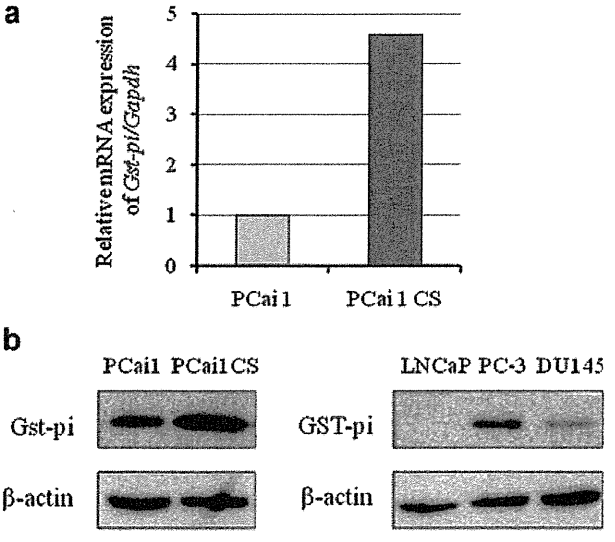

Fig. 2. Gst-pi expressions in PCai1. PCai1 in the CS-FBS medium (PCai1 CS) had higher expression levels of Gst-pi in RT-PCR (**a**) and Western blot (**b**) compared to cells in normal medium. Expressions of GST-pi in PC3 and DU145 were confirmed.

counted on days 3 and 5, and measurement of ROS level was performed as described above.

RESULTS

Establishment of an Androgen-Independent Prostate Cancer Cell Line

Our newly established androgen independent prostate cancer cell line, PCai1 (Fig. 1a), can survive in androgen-free DMEM with 10% CS-FBS. The cells showed intense nuclear immunohistochemical staining for AR in normal medium containing androgen (Fig. 1a). PCai1 and a human prostate cancer cell line LNCaP showed similar expressions of AR (Fig. 1b). The WST-1 assay revealed that cell growth was enhanced by 1–10 nM of DHT (Fig. 1c), so this cell line was androgen-independent and androgen-sensitive.

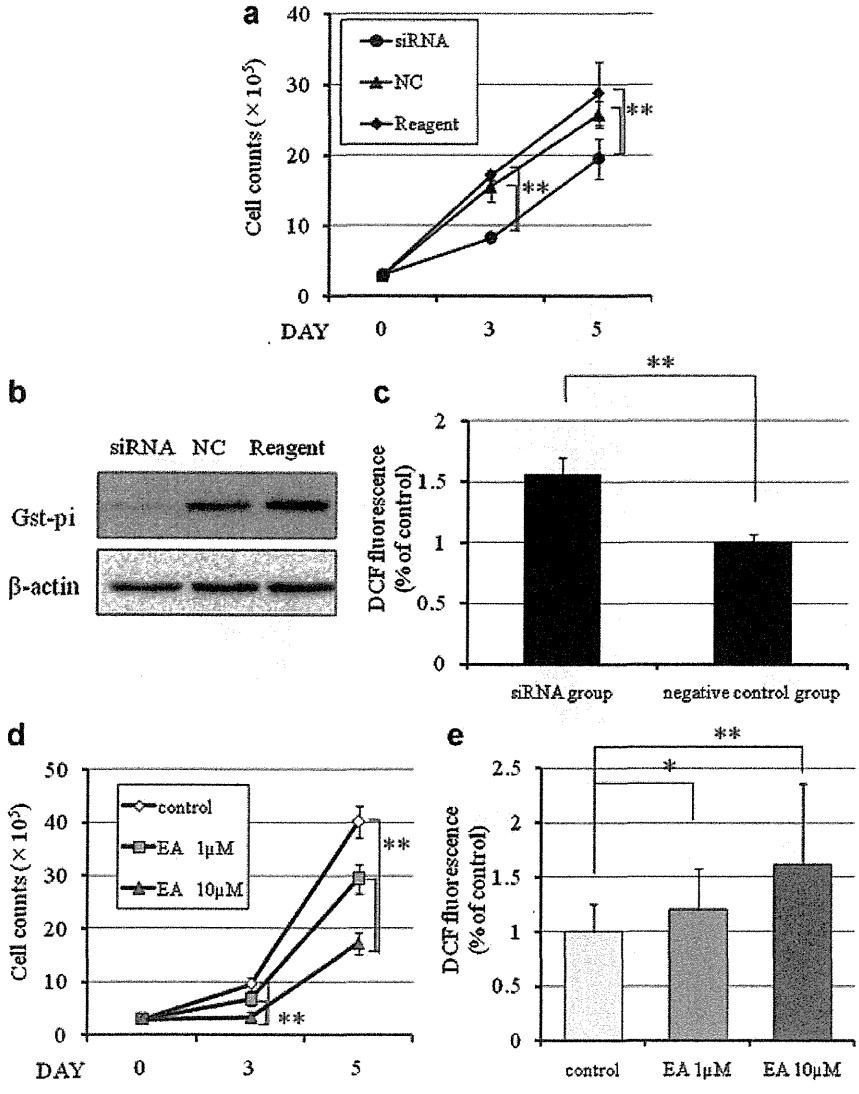

Fig. 3. Gst-pi siRNA treatment in PCai1 cells in CS-FBS medium. PCai1 cells in CS-FBS medium were treated with *Gst-pi*-siRNA. Significant growth inhibition ($^{**}P < 0.001$) was observed in the *Gst-pi*-siRNA treated PCai1 cells in CS-FBS medium (**a**). Gst-pi expression was markedly decreased in *Gst-pi*-siRNA group, while negative control (NC) group and reagent group had clearly detectable Gst-pi signals (**b**). DCFH assay revealed that ROS was significantly higher in *Gst-pi*-siRNA treatment group at day 3 after transfection ($^{**}P < 0.001$, **c**). At days 3 and 5, the numbers of PCai1 cells were counted after treatment with control, and 1 μM, 10 μM ethacrynic acid (EA). The suppression of proliferation was statistically significant by treatment of 1 or 10 μM ($^{**}P < 0.001$, **d**). DCFH assay revealed that the concentration dependence of ROS was higher in the EA treatment groups ($^{*}P < 0.05$, $^{**}P < 0.001$, **e**).

The Gst-pi Expression in PCai1 Cells

PCai1 cells in normal medium had stable expressions of Gst-pi in mRNA and protein levels. When PCai1 cells were cultured in CS-FBS medium, Gst-pi expressions were enhanced in mRNA and protein levels (Fig. 2). As reported previously [11], in human prostate cancer cells GST-pi expression was higher in the androgen-independent cell lines (PC3, DU145) compared with an androgen-dependent cell line (LNCaP). These results indicate that Gst-pi expression is higher in androgen-independent prostate cancer than those that are androgen-dependent.

Gst-pi siRNA Transfection and ROS Signals

To examine the role of Gst-pi expression for ROS signaling in PCai1 cells, *Gst-pi* expression was attenuated by RNAi. The suppression of proliferation of PCai1 cells in CS-FBS medium was statistically significant in *Gst-pi*-siRNA treated cells, but not in *Gst-pi*-negative control cells (Fig. 3a). Western blot analysis revealed Gst-pi protein expression has been inhibited by siRNA for 5 days after transfection (Fig. 3b). DCFH assay revealed that the intracellular ROS levels were significantly higher in the *Gst-pi*-siRNA treatment group than in *Gst-pi*-negative control group (Fig. 3c). Next, to examine whether Gst-pi directly affects modification of cell proliferation and production of ROS, PCai1 cells were treated with EA, a glutathione S-transferase pi inhibitor. As expected, proliferation of PCai1 was significantly inhibited by 1 and 10 μM EA compared with the non-treated control (Fig. 3d). Intracellular ROS levels were also significantly higher in the EA treatment group in a concentration-dependent manner (Fig. 3e).

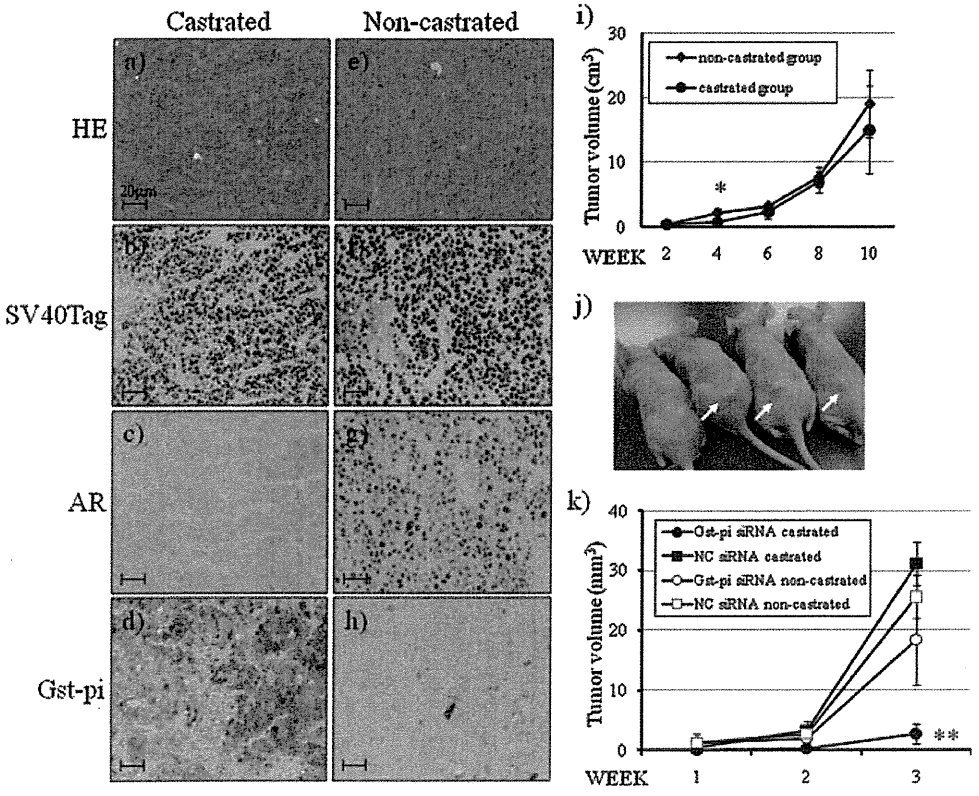

Fig. 4. Representative histopathological appearance of subcutaneous PCai1 tumor in nude mice. **a–d** shows the tumors in the castrated mice and **e–h** show the tumors in the non-castrated mice. SV40 Tag was stained to confirm origin from theTRAP prostate tumor (b,f). Non-castrated mice showed nuclear staining of AR (g), whereas castrated mice showed cytoplasmic staining (c), indicating non-active receptor function. The staining of Gst-pi was higher in castrated group (d) than in non-castrated group (h). The sequential changes are shown of subcutaneous PCai1 tumor volumes (**i**) (1×10^5 cells, n = 4 each, $^*P < 0.05$). Representative subcutaneous tumors at 2 weeks after injection in castrated or non-castrated groups (**k**, left: *Gst-pi* siRNA group with castration, second from the left: negative control siRNA group with castration, third from the left: *Gst-pi* siRNA group with non-castration, right: negative control siRNA group with non-castration, white arrow: tumor). **j**: Mean tumor volumes after subcutaneous injections (1×10^5 cells, n = 5 each). Interference of *Gst-pi* expression significantly inhibited tumor cell proliferation in castrated group compared with the corresponding negative control siRNA group ($^{**}P < 0.001$).

Prostate Cancer Subcutaneous Tumor Model

For investigation of tumorigenesis, PCai1 cells were transplanted subcutaneously in nude mice. Successful growth was seen in both castrated and non-castrated mice. The tumor sizes between the two groups lacked significance (Fig. 4i). Transplanted PCai1 cells had strong nuclear SV40 Tag expression, and demonstrated intense nuclear AR staining in the non-castrated group. In contrast, AR expression had changed from the nucleus to the cytoplasm in the castrated mice indicated not functional (Fig. 4a–h).

Prostate Cancer Orthotopic Transplanted Model

Whether or not they were castrated, the PCai1 cells grew in the prostate site in nude mice forming tumors which frequently metastasized to the lung and lymph nodes in nude mice (Fig. 5a–c and Table I). However, the mice could not survive more than 6 weeks because of urinary retention resulting from the tumor growth. Histopathologically, the prostate tumors in mice had similar characteristics as poorly differentiated prostate adenocarcinomas in human.

Intravenous Transplanted Prostate Cancer Cells

With injections of PCai1 cells into the tail veins of nude mice, metastatic tumors were frequently observed in the lungs and bones (Fig. 5g,h and Table I). Immunocytochemically, the SV40 Tag signals were intense in nuclei of PCai1 cells in vitro and in vivo of the metastasized tumor cells. All of the bone metastases were found in the lumbar vertebrae.

Regulation of Castration-Resistant Cell Growth of PCai1 by Gst-pi In Vivo

In the subcutaneous PCai1 tumors, Gst-pi expression was significantly higher in the castrated group (Fig. 4d) than in the non-castrated group (Fig. 4h) without changes in expressions of SV40 Tag (Fig. 4b,f). To evaluate roles of Gst-pi in castration-resistant cell proliferation, *Gst-pi* siRNA transfected PCai1 cells were transplanted subcutaneously in castrated or normal nude mice. Knock down of *Gst-pi* expression of PCai1 significantly inhibited tumor growth of PCai1 compared to negative controls in castrated mice. On the other hand, *Gst-pi* expression did not affect tumor growth in non-castrated mice (Fig. 4j,k).

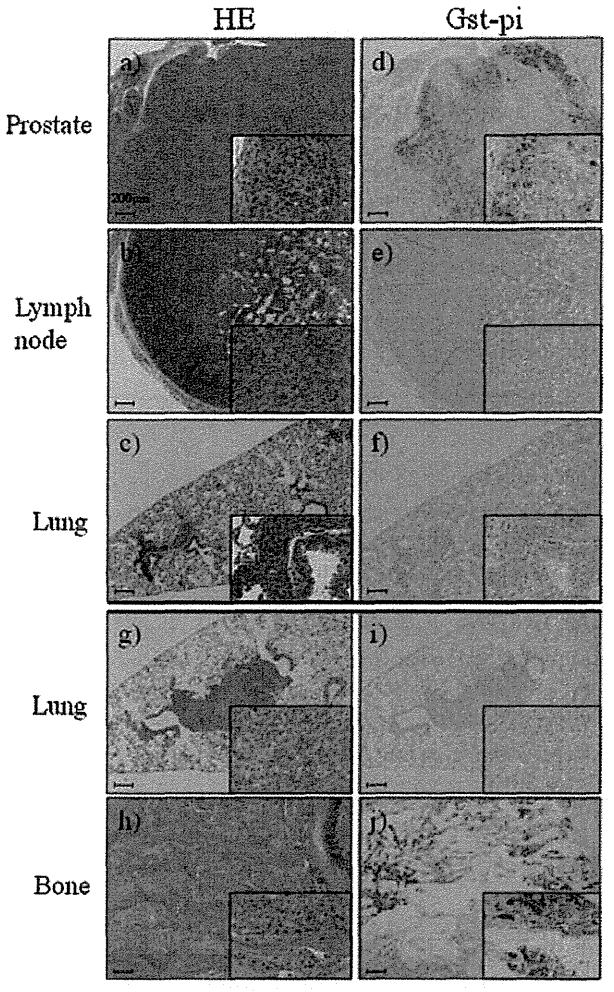

Fig. 5. Representative histopathological appearance and immunohistochemical analysis in orthotopic transplantations and tail vein injections of PCai1 cells. **a–f** show the prostate tumor and metastatic lesions 6 weeks after orthotopic transplantation of PCai1 in castrated nude mice and **g–j** show lung and bone metastatic lesions from tail vein injections of PCai1 cells 9 weeks after injection. HE staining showed that all of the tumors and metastatic lesions induced by PCai1 cells are histopathologically similar to human cases, and these lesions are compatible with poorly differentiated adenocarcinomas (a,b,c,g,h). As for the orthotopic model, the staining of Gst-pi in the prostate was higher in castrated mice (d) than in non-castrated mice (data not shown), and metastatic lesions in lymph node (e) and in lung (f) were not detected by Gst-pi staining. In contrast, Gst-pi positive staining in bone metastatic lesions was apparent (j), but in lung metastatic lesions Gst-pi positive staining was not detectable in tail vein injection models (i).

Immunohistochemical Analysis for Gst-pi in Prostate Cancer Metastatic Models

In the orthotopic in vivo model, Gst-pi showed high expression in the prostate, but no expression in

TABLE I. Frequency of Metastasis by PCai1 Cell Line

Transplantation	Castration	Sacrifice (weeks)	No. of mice	Primary tumor (%)	Metastasis (%)		
					Lymph node	Lung	Bone
Subcutaneous	–	10	4	100	–	–	–
	+	10	4	100	–	–	–
Orthotopic (prostate)	–	2	2	100	0	0	0
		5	3	100	100	33	0
	+	2	2	50	0	0	0
		6	3	100	100	75	0
Tail vein	–	5	5	–	40	80	20
		9	5	–	80	100	40

metastatic sites of lung and lymph nodes (Fig. 5d–f). However, the tumor cells injected in the tail veins resulted in tumor masses in the bone with high Gst-pi expressions (Fig. 5j). In lung (Fig. 5i) and lymph nodes, metastatic tumors did not express Gst-pi similar to that observed for lymph nodes and lung metastatic cells in the orthotopic model. These observations suggest that Gst-pi has different expression levels according to metastatic sites.

DISCUSSION

To elucidate the mechanisms of prostate cancer progression, and metastasis, physiologically relevant models are essential for understanding the human disease. Prostate cancer in the TRAP model showed marked epithelial proliferation with formation of irregular glands and luminal bridging to give a cribriform pattern, and their nuclei demonstrated enlargement and severe atypia [8]. These lesions are compatible with what are seen in human adenocarcinomas. Because of the biological complexity, bone metastatic models for prostate cancer are limited [22]. In the bone metastatic sites in our model, osteolytic areas mixed with osteoblastic areas were recognized that are similar to human cases. Therefore, our model may contribute useful information for understanding the mechanisms of prostate cancer metastasis.

The intracellular redox state balances oxidant production and antioxidant capacity of the cells based on a variety of antioxidant enzymes such as superoxide dismutase, catalase, glutathione peroxidase, and GST-pi. The glutathione redox system acts in concert to provide a coordinated network of protection against ROS accumulation and oxidative damage [23–25]. GST-pi is directly responsible for the elimination of electrophilic oxidants [23,24] especially in cancer cells characterized by rapid proliferating activity and with massive endogenous production of ROS [17].

GST-pi was usually silenced by methylation in human prostate cancer cells. However, with the acquisition of androgen-independency, our present data suggested that prostate cancer might have protective mechanisms against ROS by GST-pi signals. In our previous data, the expression level of *Gst-pi* was higher in transplantable tumors that were androgen-independent than in those that were androgen-dependent [11]. PCai1 cells in androgen-free medium had higher protein expressions of Gst-pi than in androgen-containing medium, and PCai1 tumors had higher Gst-pi expressions in castrated mice than in control mice with subcutaneous tumors and orthotopic prostate tumors in vivo. These data suggest that Gst-pi can regulate cancer cell growth by adapting to the environment. Silencing of *Gst-pi* caused significant growth inhibition of PCai1 cells, and DCFH assay revealed that intracellular ROS was significantly elevated in *Gst-pi*-siRNA and Gst-pi inhibitor treated groups. These results suggested that Gst-pi plays an important role in cell growth against ROS in PCai1 cells.

According to previous reports [26,27], the level of Gst-pi can change in response to general cellular stress. Therefore, to establish that the high expression of Gst-pi was not a reflection of cellular stress, PCai1 transplantation was performed in castrated and normal nude mice with iRNA strategy for *Gst-pi*. As a result, tumor growth of PCai1 was significantly inhibited by silencing *Gst-pi* in castrated nude mice. Therefore, Gst-pi may be necessary in androgen-independent cell growth.

Immunohistochemical analysis revealed that Gst-pi expression in subcutaneous tumors and prostate tumors in orthotopic transplants was significantly increased by castration. On the other hand, lymph nodes and lung metastatic lesions had no expression of Gst-pi. Interestingly, Gst-pi expression of the bone metastatic lesions had higher expression levels than other lesions. These findings show that Gst-pi may be

a novel therapeutic protein that can be targeted for bone metastasis.

Our newly established prostate cancer cell line PCai1, derived from the well-characterized TRAP model, may be valuable in an animal model to study the progression and metastasis of prostate cancer, and for preclinical tests of new and innovative therapeutic agents.

In summary, using our newly established prostate cancer cell line PCai1 and the metastatic models, Gst-pi expressions were shown to have important roles in prostate cancer growth and organ specific metastasis.

ACKNOWLEDGMENTS

This work was supported in part by a Grant-Aid from the Ministry of Education, Culture, Sports Science and Technology of Japan, by a Grand-Aid for Cancer Research from the Ministry of Health, Labor and Welfare of Japan, and by a Grant-Aid for Ono Pharmaceutical Co., Ltd.

REFERENCES

1. Gronberg H. Prostate cancer epidemiology. Lancet 2003; 361(9360):859–864.
2. Huggins C. Endocrine-induced regression of cancers. Cancer Res 1967;27(11):1925–1930.
3. Petrylak DP, Tangen CM, Hussain MH, Lara PN Jr, Jones JA, Taplin ME, Burch PA, Berry D, Moinpour C, Kohli M, Benson MC, Small EJ, Raghavan D, Crawford ED. Docetaxel and estramustine compared with mitoxantrone and prednisone for advanced refractory prostate cancer. N Engl J Med 2004;351(15): 1513–1520.
4. Schurko B, Oh WK. Docetaxel chemotherapy remains the standard of care in castration-resistant prostate cancer. Nat Clin Pract Oncol 2008;5(9):506–507.
5. Oh WK, Kantoff PW. Docetaxel (Taxotere)-based chemotherapy for hormone-refractory and locally advanced prostate cancer. Semin Oncol 1999;26(5 Suppl 17):49–54.
6. Shirai T. Significance of chemoprevention for prostate cancer development: Experimental in vivo approaches to chemoprevention. Pathol Int 2008;58(1):1–16.
7. Shirai T, Takahashi S, Cui L, Futakuchi M, Kato K, Tamano S, Imaida K. Experimental prostate carcinogenesis—Rodent models. Mutat Res 2000;462(2–3):219–226.
8. Asamoto M, Hokaiwado N, Cho YM, Takahashi S, Ikeda Y, Imaida K, Shirai T. Prostate carcinomas developing in transgenic rats with SV40 T antigen expression under probasin promoter control are strictly androgen dependent. Cancer Res 2001;61(12):4693–4700.
9. Said MM, Hokaiwado N, Tang M, Ogawa K, Suzuki S, Ghanem HM, Esmat AY, Asamoto M, Refaie FM, Shirai T. Inhibition of prostate carcinogenesis in probasin/SV40 T antigen transgenic rats by leuprorelin, a luteinizing hormone-releasing hormone agonist. Cancer Sci 2006;97(6):459–467.
10. Tang M, Ogawa K, Asamoto M, Hokaiwado N, Seeni A, Suzuki S, Takahashi S, Tanaka T, Ichikawa K, Shirai T. Protective effects of citrus nobiletin and auraptene in transgenic rats developing adenocarcinoma of the prostate (TRAP) and human prostate carcinoma cells. Cancer Sci 2007;98(4):471–477.
11. Hokaiwado N, Takeshita F, Naiki-Ito A, Asamoto M, Ochiya T, Shirai T. Glutathione S-transferase Pi mediates proliferation of androgen-independent prostate cancer cells. Carcinogenesis 2008;29(6):1134–1138.
12. Nelson WG, De Marzo AM, DeWeese TL. The molecular pathogenesis of prostate cancer: Implications for prostate cancer prevention. Urology 2001;57(4 Suppl 1):39–45.
13. Pathak S, Singh R, Verschoyle RD, Greaves P, Farmer PB, Steward WP, Mellon JK, Gescher AJ, Sharma RA. Androgen manipulation alters oxidative DNA adduct levels in androgen-sensitive prostate cancer cells grown in vitro and in vivo. Cancer Lett 2008;261(1):74–83.
14. Miyake H, Hara I, Kamidono S, Eto H. Oxidative DNA damage in patients with prostate cancer and its response to treatment. J Urol 2004;171(4):1533–1536.
15. Finkel T, Holbrook NJ. Oxidants, oxidative stress and the biology of ageing. Nature 2000;408(6809):239–247.
16. Nose K. Role of reactive oxygen species in the regulation of physiological functions. Biol Pharm Bull 2000;23(8):897–903.
17. Sauer H, Wartenberg M, Hescheler J. Reactive oxygen species as intracellular messengers during cell growth and differentiation. Cell Physiol Biochem 2001;11(4):173–186.
18. Feig DI, Reid TM, Loeb LA. Reactive oxygen species in tumorigenesis. Cancer Res 1994;54(7 Suppl):1890s–1894s.
19. Dakubo GD, Parr RL, Costello LC, Franklin RB, Thayer RE. Altered metabolism and mitochondrial genome in prostate cancer. J Clin Pathol 2006;59(1):10–16.
20. Chomyn A, Attardi G. MtDNA mutations in aging and apoptosis. Biochem Biophys Res Commun 2003;304(3):519–529.
21. Ripple MO, Henry WF, Rago RP, Wilding G. Prooxidant-antioxidant shift induced by androgen treatment of human prostate carcinoma cells. J Natl Cancer Inst 1997;89(1):40–48.
22. Singh AS, Figg WD. In vivo models of prostate cancer metastasis to bone. J Urol 2005;174(3):820–826.
23. Finkel T. Oxidant signals and oxidative stress. Curr Opin Cell Biol 2003;15(2):247–254.
24. Kohen R, Nyska A. Oxidation of biological systems: Oxidative stress phenomena, antioxidants, redox reactions, and methods for their quantification. Toxicol Pathol 2002;30(6):620–650.
25. Oberley LW, Buettner GR. Role of superoxide dismutase in cancer: A review. Cancer Res 1979;39(4):1141–1149.
26. Morel F, Fardel O, Meyer DJ, Langouet S, Gilmore KS, Meunier B, Tu CP, Kensler TW, Ketterer B, Guillouzo A. Preferential increase of glutathione S-transferase class alpha transcripts in cultured human hepatocytes by phenobarbital, 3-methylcholanthrene, and dithiolethiones. Cancer Res 1993;53(2):231–234.
27. Thimmulappa RK, Mai KH, Srisuma S, Kensler TW, Yamamoto M, Biswal S. Identification of Nrf2-regulated genes induced by the chemopreventive agent sulforaphane by oligonucleotide microarray. Cancer Res 2002;62(18):5196–5203.

The Prostate 72:1559–1572 (2012)

Therapeutic Targeting of Angiotensin II Receptor Type I to Regulate Androgen Receptor in Prostate Cancer

Satoru Takahashi,[1]* Hiroji Uemura,[2] Azman Seeni,[1,3] Mingxi Tang,[1,4] Masami Komiya,[1] Ne Long,[1] Hitoshi Ishiguro,[2] Yoshinobu Kubota,[2] and Tomoyuki Shirai[1]

[1]*Department of Experimental Pathology and Tumor Biology, Nagoya City University Graduate School of Medical Sciences, Nagoya, Japan*
[2]*Department of Urology, Yokohama City University Graduate School of Medicine, Yokohama, Japan*
[3]*Advanced Medical and Dental Institute, Universiti Sains Malaysia, Pinang, Malaysia*
[4]*Department of Pathology, Luzhou Medical College, Sichuan, China*

BACKGROUND. With the limited strategies for curative treatment of castration-resistant prostate cancer (CRPC), public interest has focused on the potential prevention of prostate cancer. Recent studies have demonstrated that an angiotensin II receptor blocker (ARB) has the potential to decrease serum prostate-specific antigen (PSA) level and improve performance status in CRPC patients. These facts prompted us to investigate the direct effects of ARBs on prostate cancer growth and progression.

METHODS. Transgenic rat for adenocarcinoma of prostate (TRAP) model established in our laboratory was used. TRAP rats of 3 weeks of age received ARB (telmisartan or candesartan) at the concentration of 2 or 10 mg/kg/day in drinking water for 12 weeks. In vitro analyses for cell growth, ubiquitylation or reporter gene assay were performed using LNCaP cells.

RESULTS. We found that both telmisartan and candesartan attenuated prostate carcinogenesis in TRAP rats by augmentation of apoptosis resulting from activation of caspases, inactivation of p38 MAPK and down-regulation of the androgen receptor (AR). Further, microarray analysis demonstrated up-regulation of estrogen receptor β (ERβ) by ARB treatment. In both parental and androgen-independent LNCaP cells, ARB inhibited both cell growth and AR-mediated transcriptional activity. ARB also exerted a mild additional effect on AR-mediated transcriptional activation by the ERβ up-regulation. An intervention study revealed that PSA progression was prolonged in prostate cancer patients given an ARB compared with placebo control.

CONCLUSION. These data provide a new concept that ARBs are promising potential chemopreventive and chemotherapeutic agents for prostate cancer. *Prostate 72: 1559–1572, 2012.* © 2012 Wiley Periodicals, Inc.

KEY WORDS: **angiotensin II receptor type 1; prostate cancer; androgen receptor; transgenic rat; intervention study**

Additional supporting information may be found in the online version of this article.

Grant sponsor: Ministry of Health, Labour and Welfare of Japan; Grant sponsor: Society for Promotion of Pathology of Nagoya, Japan; Grant sponsor: Ministry of Education, Culture, Science and Technology of Japan; Grant sponsor: Umehara Foundation of Yokohama Medical Group.

S. Takahashi and H. Uemura contributed equally to this work.

Conflict of Interest: None.

*Correspondence to: Dr. Satoru Takahashi, 1 Kawasumi, Mizuho-cho, Mizuho-ku, Nagoya 467-8601, Japan.
E-mail: sattak@med.nagoya-cu.ac.jp

Received 28 September 2011; Accepted 15 February 2012
DOI 10.1002/pros.22505
Published online 16 March 2012 in Wiley Online Library (wileyonlinelibrary.com).

INTRODUCTION

Prostate cancer has become the most common malignancy in men in western countries such as Europe and the United States while its incidence is low in Asian countries. It has been estimated that there will be approximately 240,890 new cases of prostate cancer and 33,720 deaths from prostate cancer in the United States in 2011 [1], and the prevalence of prostate cancer has also been increasing in Japan [2]. Androgen ablation therapy is widely accepted and carried out for prostate cancers because androgens are essential for the development and growth of normal prostate and prostate cancer cells [3]. However, outgrowth of hormone-independent cancer cells occurs within several years and eventually leads to a fatal outcome in many cases [4].

Accumulating evidence suggests that the renin-angiotensin system (RAS) is involved in maintenance of blood pressure as well as progression of various cancers, such as breast, lung, kidney, stomach, colorectum, ovary, and bladder [5]. Angiotensin II is a main effector molecule of the RAS and is an octapeptide hormone with diverse biological activity through binding to typical G protein-coupled receptors, angiotensin II receptor type 1 (AT1R) and type 2 (AT2R). AT1R is expressed in diverse adult tissues and mediates cell proliferation, migration, angiogenesis, and inflammatory responses via G protein-dependent and independent signaling including the MAPK and STAT signal pathways [6]. AT2R is predominantly expressed at a high level in the fetus, and its expression is low in adult tissues, being detectable in heart, kidney, pancreas, adrenal gland, uterus, ovary, and brain [7]. In contrast to AT1R, AT2R has been shown to exert an antagonistic effect against many AT1R-mediated actions [5,8]. Recent studies have demonstrated that an angiotensin II receptor blocker (ARB) has the potential to decrease serum prostate-specific antigen (PSA) level and improve performance status in some patients with castration-resistant prostate cancer (CRPC) [9,10]. Moreover, expression of AT1R and angiotensinogen in CRPC was significantly higher than that in normal prostate tissue or hormone-naive prostate cancer [11]. These facts prompted us to confirm the direct effects of ARBs on prostate cancer and investigate the mechanisms of their suppression of prostate cancer growth and progression.

We have established a transgenic rat for adenocarcinoma of prostate (TRAP) model bearing a probasin promoter/simian virus 40 (SV40) T antigen construct, which features development of high-grade prostatic intraepithelial neoplasia (PIN) from 4 weeks of age and well-moderately differentiated adenocarcinoma with high incidences by 15 weeks of age [12,13]. These characteristics of TRAP have been shown to be very suitable for evaluation of strategies for chemoprevention and treatment with ARBs in vivo.

Here, we showed that ARBs attenuate prostate cancer development in TRAP rats and androgen receptor (AR)-mediated transcriptional activity in human prostate cancer cells. Also, we showed that an ARB delayed PSA progression in patients with local recurrence after radical prostatectomy clinically.

MATERIALS AND METHODS

Chemicals, Reagents, Plasmids, and Cell Line

Telmisartan was provided by Boehringer Ingelheim (Ingelheim, Germany) and candesartan was from Takeda Pharmaceutical Co. Ltd. (Osaka, Japan). MG132 was purchased from Calbiochem (EMD Biosciences, Inc., San Diego, CA), diarylpropionitrile (DPN) from Tocris Bioscience (Bristol, UK), and biochanin A from Sigma (St. Louis, MO). The PSA promoter reporter construct (pGL3/PSA promoter) was donated by Dr. Chawnshang Chang, University of Rochester Medical Center. An expression vector for human ERβ (pCXN2/ERβ) was provided by Dr. Masami Muramatsu (Saitama Medical University, Japan). To generate an expression vector for FLAG-tagged human AR (pCMVTag/hAR), the human AR open reading frame was amplified by PCR and cloned into the pCMV-Tag2 vector at *Bam*HI/*Xho*I sites. The human prostate cancer cell lines LNCaP (androgen-dependent) and VCaP (androgen-independent), and the non-tumorigenic prostate epithelial cell line RWPE-1 were obtained from the American Type Culture Collection (Manassas, VA). Four androgen-independent (AI) sublines derived from LNCaP were established after seven repeated cycles of incubation using the following culture medium; RPMI1640 containing 10% FBS for 5–7 days or RPMI1640 containing 10% charcoal-stripped FBS for 2–3 weeks. AI sublines were designated AI-1, -5, -5s, and -8, respectively (Fig. S1A,B).

Animals

Male heterozygous TRAP rats established in our laboratory with a Sprague–Dawley genetic background were used in the present study. They were housed at three animals per cage on wood-chip bedding in an air-conditioned animal room at 23 ± 2°C and 50 ± 10% humidity. Food and tap water were available ad libitum.

Experimental Protocol

Experiment 1. A total of 36 heterozygous male TRAP rats of 3 weeks of age were randomly divided into

three groups. Rats in Group 1 as a control received basal diet and tap water. The rats in Groups 2 and 3 continuously received 2 or 10 mg/kg/day telmisartan in drinking water for 12 weeks, respectively.

Experiment 2. A total of 48 heterozygous male TRAP rats of 3 weeks of age were randomly divided into four groups. Rats in Group 1 as a control received basal diet and tap water. The rats in Groups 2–4 continuously received 2 or 10 mg/kg/day candesartan or 10 mg/kg/day telmisartan in drinking water for 12 weeks, respectively.

In both experiments, measurement of blood pressure was performed at weeks 4, 7, and 11, and the experiments were terminated at week 15. The prostate was removed and fixed in formalin. A part of the prostate glands was immediately frozen in liquid nitrogen and stored at −80°C until processed. Testosterone and estrogen levels in serum were analyzed using radioimmunoassay by a commercial laboratory (SRL, Inc., Tokyo, Japan). The present experiments were performed under protocols approved by the Institutional Animal Care and Use Committee of Nagoya City University Graduate School of Medical Sciences.

Assessment of Prostate Neoplastic Lesion Development

Neoplastic lesions in the prostate gland of TRAP rats were evaluated as previously described [14]. Briefly, neoplastic lesions were classified into three types: low-grade PIN (LG-PIN), high-grade PIN (HG-PIN), and adenocarcinoma. The relative numbers of acini with the histological characteristics of each type, that is, LG-PIN, HG-PIN, and adenocarcinoma, were quantified by counting the total acini in each prostatic lobe.

Immunoblot Analysis

Immunoblot analysis was performed as described previously [15]. Briefly, frozen ventral prostate tissues were homogenized in RIPA buffer (150 mM NaCl, 50 mM Tris–HCl (pH 8.0), 1% NP-40, 0.5% sodium deoxycholate, 0.1% SDS, 1 mM phenylmethylsulphonyl fluoride, 1 mM sodium orthovanadate, and protease inhibitor cocktail [Complete, Roche]). The antibodies used were cyclin D1 (Oncogene Science, Cambridge, MA), caspases 3, 7, and 9, Erk 1/2 and phophs-Erk1/2, p38 MAPK and phospho-p38 MAPK (Cell Signaling Technology, Danvers, MA), AR and SV40 T antigen (Santa Cruz Biotechnology, Inc., Santa Cruz, CA), VEGF (IBL Co. Ltd., Fujioka, Japan) and β-actin (Sigma). The intensity of each band was measured using Image J 1.440 (National Cancer Institute, Bethesda, MD).

Immunohistochemistry

Deparaffinized sections were incubated with diluted antibodies for Ki-67 (Novocastra Laboratories Ltd., Newcastle, UK), SV40 T antigen (Santa Cruz Biotechnologies), phospho-p38 MAPK (Thr180/Tyr182), and cleaved caspase 3 (Asp175: Cell Signaling Technology, Danvers, MA). Apoptotic cells in the prostate were detected using an In Situ Apoptosis Detection Kit (TUNEL method) according to the manufacturer's instructions (Takara Bio Inc., Ohtsu, Japan). Labeling indices for Ki-67, TUNEL, cleaved caspase 3 or phospho-p38 MAPK were generated by counting over 1,000 cells mainly in HG-PIN under microscope at high magnification and they were expressed as numbers of positive cells per 100 cells. To evaluate the effect of telmisartan against angiogenesis, microvessels were detected using anti-factor 8-related antigen (DAKO, Glostrup, Denmark).

Cell Proliferation Assay

Cell proliferation of prostate cancer cell lines was assessed by 4-[3-(4-iodophenyl)-2-(4-nitrophenyl)-2H-5-tetrazolio]-1,3-benzene disulfonate tetrazolium salt (WST-1) assay (Roche Applied Science, Mannheim, Germany). Briefly, cells were seeded in 96-well plates at 1×10^4 cells/well in 200 μl of culture media. ARBs or ERβ agonists were added 24 hrs after seeding and incubated for 3 days. WST-1 reagent was added to each well with incubation for 60 min at 37°C, and then each well were measured for absorbance at 430 nm.

Ubiquitylation Assay

LNCaP cells were transfected with Flag-tagged human AR (pCMVTag/hAR) using Nucleofector II (Amaxa AG, Koeln, Germany), seeded into a 6-well plate and incubated for 24 hr. Cells were treated with ARBs and/or 1 μM MG132 for 24 hr, and then lysed with RIPA buffer supplemented with COMPLETE protease inhibitor cocktail (Roche Diagnostics GmbH, Mannheim, Germany). The extracts were immunoprecipitated with anti-Flag antibody (Sigma) and protein G sepharose (GE Healthcare Bio-sciences AB, Uppsala, Sweden) for 3 hr at 4°C. After washing the agarose with RIPA buffer, Laemmli sample buffer was directly added to the agarose and heated to 85°C for 10 min. Samples were subjected to immunoblot analysis using anti-ubiquitin antibody (Santa Cruz).

Reporter Gene Assay

LNCaP cells were transfected with the pGL3/PSA promoter using Nucleofector II. Twenty-four hours after transfection, 5 nM DHT and/or ARB was added.

Cells were lysed with the buffer supplied in the kit 72 hr after transfection. The luciferase assay was conducted using the dual-luciferase reporter assay system (Promega Corporation, Madison, WI) according to manufacturer's protocol. Data shown represent the mean and standard deviation of four independent data points.

Microarray Analysis

Total RNA was isolated from ventral prostate tissues as en bloc by phenol–chloroform extraction (ISOGEN, Nippon Gene Co. Ltd., Toyama, Japan), and fluorescent cRNA amplification was performed using a Low RNA Input Fluorescent Linear Amplification kit (Agilent Technologies, Palo Alto, CA) according to the manufacturer's instruction. Total RNA from ventral prostate of F344 rat was used as a reference RNA. Quality of total and amplified cRNAs was examined with a high-resolution electrophoresis system, Agilent 2100 Bioanalyzer (Agilent Technologies). Gene expression analysis was performed using a Whole Rat Genome oligo DNA microarray (4 × 44k; Agilent Technologies). The slides were hybridized with Cy3- or Cy5-labeled cRNA for 16–18 hr at 60°C, washed in 0.5 × SSC/0.01% SDS buffer for 5 min at room temperature, then 0.06 × SSC buffer for 2 min, and desiccated with a centrifuge. The slides were scanned with a DNA Microarray Scanner (Agilent Technologies) at two wavelengths to detect emission from both Cy3 and Cy5. Genes with significantly different expression levels were revealed by Significance Analysis of Microarray (ver 2.0; delta = 0.34; http://www-stat.stanford.edu/~tibs/SAM/).

Real-Time RT-PCR

Total RNA was isolated from ventral prostate tissues as en bloc using an RNeasy Mini kit (Qiagen, Valencia, CA). Total RNAs were reverse-transcribed with the Thermoscript first-strand synthesis system (Invitrogen Corporation, Carlsbad, CA), and real-time RT-PCR was performed using a LightCycler (Roche Diagnostics GmbH). The oligonucleotides listed in Table S1 as primers.

RNA-Interference

siRNAs were designed and obtained from RNAi Co. Ltd. (Tokyo, Japan), AR, ERβ and control siRNA sequences were 5′-GAGGAGCUUUCCAGAAUCUGU-3′, 5′-GGAAAUGCGUAGAAGGAAUUC-3′ and 5′-GUACCGCACGUCAUUCGUAUC-3′, respectively. LNCaP cells were transfected with siRNAs using Nucleofector II.

Statistical Analysis

Differences in incidences or means between groups were determined by analysis of variance (ANOVA), followed by the Dunn' multiple comparison test or Dunnett's post-hoc test with GraphPad Prism (version 5.0c; GraphPad Software, Inc., La Jolla, CA), respectively.

Intervention Study

After Institutional Review Board approval was obtained, data from 234 patients undergoing radical prostatectomy (RP) at Yokohama City University Hospital and Center Hospital from March 1999 to July 2007 were entered into our database. Biochemical failure (BCF) was defined as a single PSA level of >0.2 ng/ml. The PSA-doubling time (DT) was calculated by log-linear regression and analyzed, respectively, as from the nadir PSA level after RP up to 0.2 ng/ml, and from 0.2 ng/ml to about 1.0 ng/ml. Briefly, PSA-DT was calculated starting with the nadir PSA value after RP, and included all PSA values up to 0.2 ng/ml used in the PSA-DT calculations, and also required patients to have a minimum of two values separated by at least 3 months, which was designated as ePSA-DT. In cases with a PSA value over 0.2 ng/ml, PSA-DT was calculated using PSA values after BCF (i.e., >0.2 ng/ml), as opposed to ePSA-DT, which was computed using all values after BCF up to about 1.0 ng/ml, at which point secondary therapy, for example, radiotherapy or hormonal therapy, was started, which was designated as aPSA-DT.

Eighteen patients were enrolled in this study. All patients underwent RP, and the specimens showed adenocarcinoma pathologically, with tumor stage T2 or T3, without lymph node metastasis (pathological stage: T2 or T3 N0M0). At BCF of PSA values, they received olmesartan (Dai-ichi Sankyo Co., Tokyo, Japan), an ARB, at 10–20 mg once daily till they received secondary therapy when their PSA values were over 1.0 ng/ml. ePSA-DT was calculated using all PSA values from the PSA nadir after RP until the start of olmesartan. Then, aPSA-DT was calculated using all PSA values after the start of olmesartan to the start of secondary therapy, at which point their PSA values were over 1.0 ng/ml. As for the control, 9 patients were not treated after RP until PSA level was over 1.0 ng/ml. ePSA-DT was calculated starting with the nadir PSA value after RP and included all PSA values up to 0.2 ng/ml, and aPSA-DT was calculated using all PSA values from BCF (>0.2 ng/ml) to over 1.0 ng/ml.

We compared ePSA-DT and aPSA-DT of olmesartan-treated patients and control patients. Also, the ratio of aPSA-DT/ePSA-DT was compared between

olmesartan-treated patients and control patients by Wilcoxon signed-rank test. Furthermore, the time to PSA progression over 1.0 ng/ml after BCF and from the nadir PSA value ($TTPP_{1.0}$) was estimated using Kaplan–Meier method and analyzed using log rank test.

RESULTS

Animal Experiment UsingTRAP Rats

Experiment 1. One rat in the control group was omitted from the effective animals because of suffering from cachexia due to the spontaneous development of leukemia. Blood pressure of TRAP rats treated with telmisartan was significantly lowered in a dose-dependent manner (Table S2). Telmisartan decreased mean body weight and increased kidney weight but did not influence the ventral prostate and liver weights (Table S2, Fig. S2A). Histologically, stromal edema was demonstrated in the kidneys of TRAP rats given telmisartan but tubular or glomerular damage was not evident (Fig. S2C). Serum levels of testosterone and estradiol were not affected by telmisartan (Table S2). In the lateral prostate, a significant decrease in the incidence of adenocarcinoma was observed (Table I). In the ventral prostate, there was a marked or partial pathologic response to telmisartan treatment, as demonstrated by a significant reduction in the amount of prostatic neoplastic lesions in TRAP rats; however, small foci of adenocarcinoma still remained, so there was no significant difference in the incidence of PIN or adenocarcinoma in the prostate of TRAP rats (Table I). Quantitative evaluation of the proportion of preneoplastic and neoplastic lesions in the prostate gland showed significant suppression of progression from LG-PIN to HG-PIN or adenocarcinoma in rats treated with telmisartan (Table II). There was a significant increase in the apoptotic index in the prostate of TRAP rats given telmisartan (Fig. 1A), although Ki-67 index was not different among the groups (Fig. 1B). In the ventral prostate, immunoblot analyses showed activation of caspases 3 and 7 and inactivation of p38 MAPK in rats treated with telmisartan, while expression of cyclin D1 was not altered in all groups (Fig. 1E). Both caspase 3 activation and decreased expression of phospho-p38 MAPK were confirmed by immunohistochemistry (Fig. 1G,I). There was no difference in the expression of AT1R in the ventral prostate between telmisartan-treated and control rats (Fig. 1K). ARB exerted suppressive effects on the growth of prostate cancer via the inhibition of angiogenesis in a tumor xenograft model [16]. The possibility that telmisartan augmented apoptosis in prostate cancer through suppression of tumor angiogenesis in TRAP rats was examined. Unexpectedly, VEGF protein expression in the ventral prostate was not altered by telmisartan treatment (Fig. S3), and there was no difference in microvessel density among the groups (Table S3).

Experiment 2. To confirm the reproducibility of the suppressive effect of telmisartan on prostate carcinogenesis, we performed an experiment with a similar design to that of experiment 1. Candesartan, a selective AT1R blocker with no PPARγ agonistic activity at usual doses, was applied for comparison with the effects of telmisartan. Body weight gain and organ weights were not affected by candesartan (Table S4, Fig. S2B). Serum levels of testosterone and estradiol were not significantly different between telmisartan and candesartan treatment (Table S4). Prostate adenocarcinomas were found only in the ventral and lateral lobes, and a significant decrease in its incidence was observed in the lateral prostate and suppression of the progression of prostatic lesions from LG-PIN to

TABLE I. Incidences of Adenocarcinoma of the Prostate Glands of TRAP Rats

Treatment	No. of rats	Ventral AC (%)	Lateral AC (%)	Dorsal AC (%)
Experiment 1				
Control	11	11 (100)	9 (82)	0
TS 2 mg/kg/day	12	11 (92)	8 (67)	0
TS 10 mg/kg/day	12	9(75)	4 (33)*	0
Experiment 2				
Control	12	12(100)	12 (100)	0
CS 2 mg/kg/day	12	12(100)	10 (83)	0
CS 10 mg/kg/day	12	11 (92)	5 (42)**	0
TS 10 mg/kg/day	12	12(100)	4 (33)**	0

TS, telmisartan; CS, candesartan; AC, adenocarcinoma.
*$P < 0.05$ versus control.
**$P < 0.01$ versus control.

TABLE II. Quantitative Evaluation of Neoplastic Lesions in Ventral Prostate of TRAP Rats Treated With ARBs

Treatment	No. of rats	LG-PIN	HG-PIN	AC
Experiment 1				
Control	11	7.2 ± 2.3	90.1 ± 2.2	2.7 ± 1.2
TS 2 mg/kg/day	12	11.9 ± 4.2*	86.7 ± 4.2	1.4 ± 0.4**
TS 10 mg/kg/day	12	12.5 ± 5.0**	85.9 ± 4.8*	1.6 ± 0.6**
Experiment 2				
Control	12	10.6 ± 4.5	83.1 ± 3.4	6.3 ± 2.8
CS 2 mg/kg/day	12	13.5 ± 5.9	82.6 ± 4.9	3.9 ± 2.1*
CS 10 mg/kg/day	12	18.4 ± 4.9**	78.9 ± 4.5	2.7 ± 1.2***
TS 10 mg/kg/day	12	22.5 ± 8.6***	75.0 ± 7.8**	2.5 ± 1.3***

Values (mean% ± SD) are the relative number of acini with histological characteristics against whole number of acini.
LG-PIN, low-grade prostatic intraepithelial neoplasia; HG, high grade; AC, adenocarcinoma; TS, telmisartan; CS, candesartan.
*$P < 0.05$ versus control.
**$P < 0.01$ versus control.
***$P < 0.001$ versus control.

HG-PIN or adenocarcinoma were found in rats given telmisartan and high-dose candesartan (Tables I and II). The numbers of apoptotic cells in both the ventral and lateral prostate of rats treated with both telmisartan and candesartan were significantly increased as compared with the controls, whereas there was no obvious difference in Ki-67 labeling index (Fig. 1C,D). Immunoblot and immunohistochemical analyses clearly demonstrated activation of caspases 3 and 7 and a tendency for inactivation of p38 MAPK in the ventral prostate of rats treated with both candesartan and telmisartan, as likewise shown in experiment 1 (Fig. 1F,H,J). There was no significant difference in AT1R expression among the groups (Fig. 1L).

Suppressive Effects of ARBs on the Expression and Transcriptional Activity of Androgen Receptor (AR)

We examined the effects of ARBs on AR expression because previous clinical studies demonstrated that ARBs have potential to decrease serum PSA level in prostate cancer patients. AR protein expression was down-regulated in the ventral prostate of TRAP rats while SV40 T antigen protein and AR mRNA expression did not differ among the groups (Fig. 2A,B). Immunohistochemical analysis revealed that all prostate epithelial cells, including neoplastic and normal-looking cells, expressed SV40 T antigen at almost similar levels (Fig. S4A). Real-time RT-PCR of the androgen responsive gene, GK11, known as an ortholog of human PSA, demonstrated significant down-regulation by ARB treatment while probasin expression levels showed no clear alteration (Fig. S4B,C). In human prostate cancer and prostate epithelial cells, all cells used in the present study expressed both AT1R and AT2R but its levels were variable (Table S5). In LNCaP cells, ARBs repressed both AR and PSA protein expression although real-time RT-PCR analysis of the AR gene showed no obvious difference among treatments (Fig. 2C,E). ARBs also suppressed both AR and PSA expression in VCaP cells, androgen-independent prostate cancer cells harboring wild type AR (Fig. 2D). The suppressive effect of ARBs on AR protein expression was blocked by the proteasome inhibitor, MG132, suggesting that a proteasome-dependent pathway is involved in ARB-induced AR protein down-regulation (Fig. 2F). Subsequent luciferase reporter assays clearly demonstrated significant inhibition of AR transcriptional activity, this finding being considered to simply reflect down-regulation of AR protein expression by ARBs (Fig. 2G).

In RWPE-1 cells, normal epithelial cells from the peripheral zone of the human prostate immortalized with human papilloma virus 18, candesartan did not affect cell growth while high-dose of telmisartan attenuated cell proliferation (Fig. S5).

Estrogen Receptor β (ERβ) Upregulation by ARBs in Prostate of TRAP Rats and Human Prostate Cancer Cell Lines

To further investigate the downstream molecule(s) of AT1R responsible for suppression of prostate carcinogenesis, we performed microarray analysis using ventral prostate tissue of TRAP rats. According to comprehensive mRNA profiling by DNA microarray, 28 genes were up-regulated and 43 were down-regulated in the telmisartan treatment group over the control (Delta = 0.340; Fig. S6). Table S6 showed significant genes detected microarray analysis. Among these genes, we focused on ERβ as one of the genes up-regulated by ARB treatment because the majority

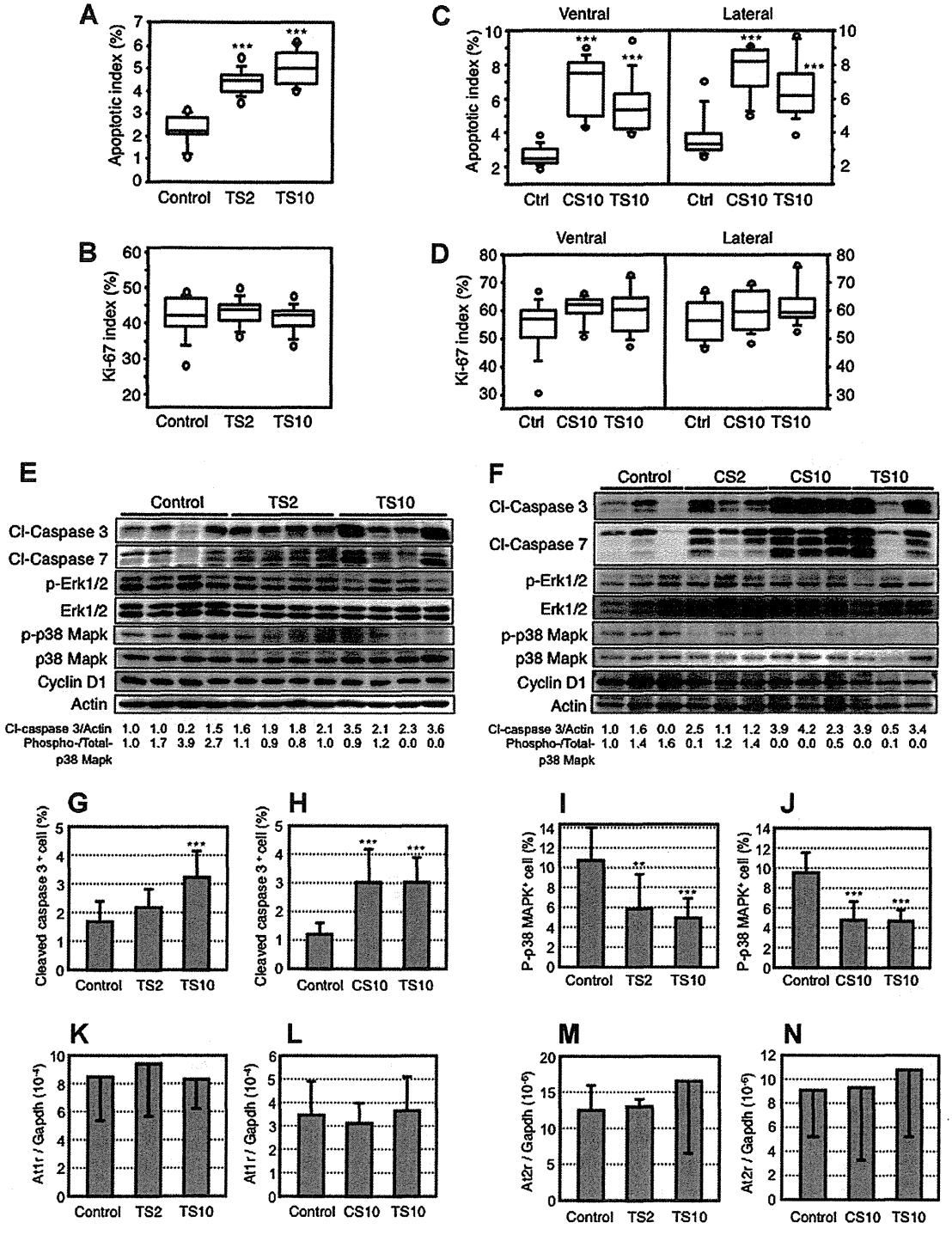

Fig. 1. Labeling indices for apoptosis (TUNEL), Ki-67 positive cells and immunoblot analysis in prostate of TRAP rats treated with ARB. Box plot data for TUNEL (**A**), Ki-67 (**B**) indices in ventral prostate in Experiment I, and TUNEL (**C**) and Ki-67 (**D**) indices in each prostatic lobe in Experiment 2. Labeling indices were counted in prostate epithelial cells of all rats and more than 1,000 cells were evaluated to give percentage values. $^{***}P < 0.001$ versus control. **E**,**F**: Immunoblots of protein lysates (20 μg) of ventral prostate in Experiment I and 2, respectively, were probed with antibodies to cleaved caspases 3 and 7, MAPKs, cyclin DI and β-actin. Quantitative data for labeling of cleaved caspase 3 (**G**,**H**) or phospho-p38 MAPK (**I**,**J**) in the ventral prostate in Experiments I and 2, respectively. Quantitative data for angiotensin II receptor type I (**K**,**L**) and type II (**M**,**N**) expression in the ventral prostate in Experiments I and 2, respectively. Data except immunoblotting were analyzed using all animal samples. **, $^{***}P < 0.01$ and 0.001 versus control. TS2 and TSI0, telmisartan 2 and 10 mg/kg/day, respectively; CS2 and CSI0, candesartan 2 and 10 mg/kg/day, respectively; Ctrl, control.

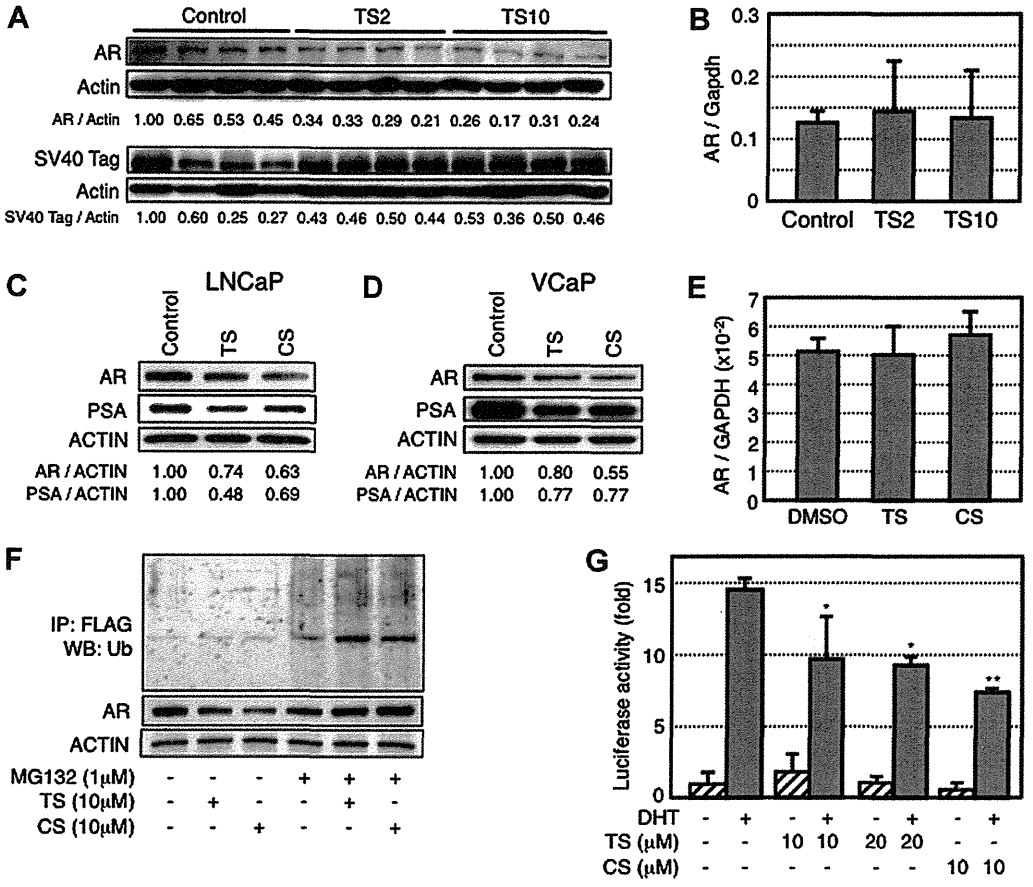

Fig. 2. Effect of ARBs on AR expression in TRAP rats or human prostate cancer cells. Immunoblot (**A**) or Real-time-RT-PCR (**B**) analysis for AR in the ventral prostate of TRAP rats. The intensity of each band was measured and normalized to actin. Data were analyzed using all animal samples and represent mean ± SD. Immunoblot analysis for AR in LNCaP (**C**) and VCaP (**D**) treated with 10 μM TS or CS for 3 days. The intensity of each band was measured and normalized to actin. **E**: Real-time RT-PCR for AR in LNCaP exposed 10 μM TS or CS for 3 days. **F**: Ubiquitylation assay for AR in LNCaP cells transfected with FLAG-tagged human AR, treated with 10 μM TS, CS and/or 1 μM MG132 for 24 hr. Protein extracts prepared from treated or untreated cells were subjected to immunoprecipitation using anti-FLAG antibody. The ubiquitylation status of AR was analyzed by immunoblotting using anti-ubiquitin antibody. **G**: Inhibition of PSA promoter luciferase activity by ARBs in LNCaP cells. Cells were transfected with both a PSA promoter reporter construct (pGL3/PSA promoter) and a control phRL-TK Renilla luciferase vector. Cells were incubated in the absence or presence of 5 nM DHT and/or ARBs for 48 hr in RPMI1640 containing 10% charcoal-stripped FBS without phenol red. Data represent the mean and standard deviation of four independent data points. $^{*},^{**}P < 0.05$ and 0.01 versus no treatment control, respectively. TS2 and TS10, telmisartan 2 and 10 mg/kg/day, respectively; CS, candesartan.

of the genes other than ERβ were involved in the regulation of blood pressure. First, we needed to confirm ERβ expression in TRAP rat prostate in both in vivo experiments, as we have done. As expected, significant elevation of ERβ mRNA was observed in the ventral prostate of TRAP rats by quantitative RT-PCR (Fig. 3A,B), and a similar phenomenon was found in LNCaP cells exposed to ARBs (Fig. 3C).

Up-Regulation of ERβ Induce Suppression of AR Transcriptional Activity and Prostate Cancer Cell Growth

Luciferase reporter assay demonstrated that forced expression of ERβ in LNCaP cells clearly inhibited AR-mediated transcriptional activity in both ligand-dependent and -independent manners (Fig. 3D). Treatment with selective ERβ agonists, diarylpropionitrile (DPN) and biochanin A, suppressed both growth and AR-mediated transcriptional activity of LNCaP cells as did ARBs (Fig. 3E,F). Immunoblot analysis revealed that selective ERβ agonists down-regulated PSA expression but AR expression was increased in LNCaP cells (Fig. 3G). Selective ERβ agonist-induced cell growth suppression was blocked by siRNA-mediated knock-down of AR expression, suggesting that the suppressive action of ERβ was via the AR signaling pathway (Fig. 3H). Knock-down of ERβ expression by siRNA did not affect on cell